of ζ/ψ and by Franz and Teepe[7] using very low values of ζ/ψ Experimental confirmation also can be obtained from analyzing a stack of skewed quarter-wave plates cut from Polaroid quarter-wave plastic sheet

Complete light-solutions for the general shell problem may be obtained with a train of matrices performing the operations of the sphere [4] The value of the approach outlined here is that a clear visual conception of complex polarization states is readily achieved; hence, the method of the sphere may be quite useful in helping to formulate approaches for final mathematical solutions

References

[1] Ramachandran, G N and Ramasehon, S , "Crystal optics," *Handbuch der Physics*, Band XXV/1, edited by S Flugge (Springer-Verlag, Berlin, 1961), pp 1–217

[2] Deschamps, G A , 'Geometrical representation of the polarization of a plane electromagnetic wave " Proc Inst Radio Engrs **39**, 540–544 (1951)

[3] Born, M and Wolf, E , *Principles of Optics* (Pergamon Press, New York, 1959), pp 29–31

[4] Schurcliff, W A , *Polarized Light* (Harvard University Press, Cambridge, Mass , 1962) pp 95–99

[5] Drucker, D C and Mindlin, R D , "Stress analysis by three dimensional photoelastic methods," J Appl Phys **11**, 724–732 (1940)

[6] Drucker, D C , "The photoelastic analysis of transverse bending of plates in the standard transmission polariscope," J Appl Mech **10**, A161–164 (1942)

[7] Franz, G and Teepe, W , "Beitrag zur spannungsoptischen untersuchung von schalen," *Selected Papers on Stress Analysis* (Chapman and Hall Ltd , London, 1961), pp 50–57

MGD Space Propulsion System for Lunar Missions

FRED SPINDLER* AND KENNETH WANG†
Curtiss-Wright Corporation,
Wood-Ridge, N J

IN a recent paper[1] Brown and Nicoll have made a mission study of arcjet and ion engines for lunar ferry missions The calculations indicated that both engines offer payload capabilities superior to the chemical and nuclear rocket propulsion systems, particularly in the case of multitrip ferry missions The present study of the mission capability for an MGD propulsion system also shows the advantage in using it for lunar ferry missions Compared with either an ion engine or arc-jet engine the MGD propulsion system yields either shorter trip duration or larger payload for equal power/weight ratio Thus, an integrated MGD space propulsion system needs to be investigated as a promising system for space exploration

In order for the results of calculation to be meaningful and comparable, a mission profile identical to that described in Ref 1 is adopted

Starting with the characteristics of the MGD propulsion system, the propulsion efficiency is obtained from the theoretical analysis of Ref 2 In Fig 1, the efficiency of the MGD propulsor is presented together with those of the ion engine and arcjet for comparison Then, for a given propulsion time the specific weight of vehicle in lb/kw can be found from the simplified rocket equation for gravity free space For a particular propulsion system the specific weights for the space vehicle components such as guidance system, structure, fuel storage, etc , can be estimated and the specific fuel weight calculated for a given I_{sp}

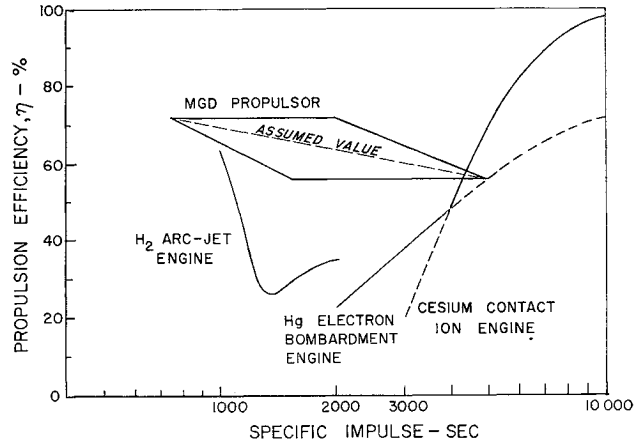

Fig 1 Comparative electric propulsion performance

Finally, the specific payload weight is obtained by subtracting the sum total of these specific weights from the specific weight of vehicle Repeated calculations for various propulsion times and specific impulse values yields a series of parametric mission performance curves showing payload fraction and power to weight ratio

In Fig 2 the payload capabilities of MGD propulsion for a round trip lunar mission are presented together with results of Ref 1 for comparison purposes The specific weights for the space vehicle components adapted in the calculations are as follows: 1) power conversion system weight, 7 lb/kw for the 1–10 mw power range; 2) power conditioning system weight, 3 lb/kw (power transmission lines, switchgear, controls, starting devices, and any requirements for power transformation or rectification); 3) propulsion system weight, 1 lb/kw; 4) guidance and control system weight = 0 3% W_o (initial weight); 5) structural weight of spacecraft = 5% of empty vehicle weight except fuel storage weight; 6) propellant weight = (propulsion time × thrust)/(I_{sp} × power); and 7) propellant storage and feed system weight = 12% of propellant weight

It can be seen that the mission capability of the MGD propulsion system lies approximately midway between that of the arcjet and the ion engine The advantages of the MGD

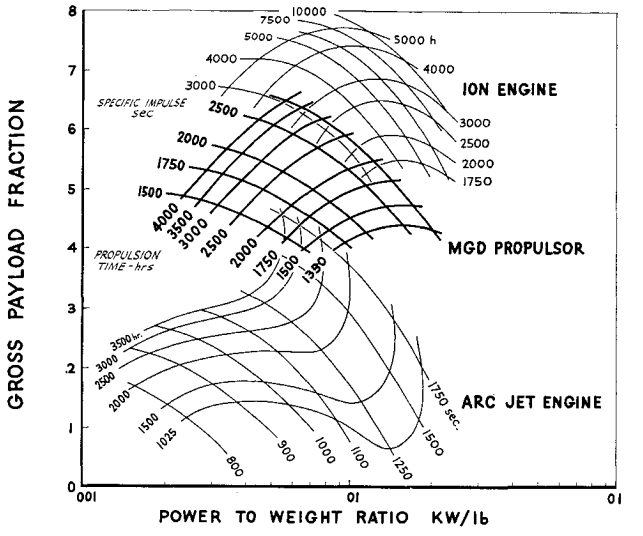

Fig 2 Payload capabilities for round-trip lunar missions

Received October 4, 1963

* Senior Engineer, Advanced Energy Conversion Department, Wright Aeronautical Division

† Project Manager, Advanced Energy Conversion Department, Wright Aeronautical Division Member AIAA

Table 1

	Payload fraction, %	Mission duration, hr	Specific impulse, sec
Arcjet	11	1025	1125
MGD	45	1500	2000
Ion engine	55	2000	3000

propulsion system over the arcjet and the ion engine, therefore, are the shorter mission duration at little sacrifice in payload, or conversely, higher payload fraction with slight increase in mission duration

As an example, with power to weight ratio at 0 01 kw/lb the values as shown in Table 1 are obtained

Table 1 clearly indicates the superior mission capability of the MGD propulsion system for lunar ferry missions Assuming a 220,000 lb initial weight, the gain in payload with the MGD propulsion system can be nearly 75,000 lb over that of the arcjet with an increase in mission duration of 475 hr On the other hand, the mission duration can be shortened by 500 hr for a slight reduction of payload (22,000 lb) as compared with the ion engine

The particular example thus proves decidedly the advantages in using MGD propulsion for lunar ferry missions

References

[1] Brown, H and Nicoll, H E, Jr, "Electrical propulsion capabilities for lunar exploration," AIAA J 1, 314–319 (1963)

[2] Brandmaier, H E, Durand, J L, Gourdine, M C, and Rubel, A, "An investigation of a one kilowatt hall accelerator," AIAA Preprint 63046 (March 1963)

Supersonic Magnus Effect on a Finned Missile

EDWARD R BENTON*
National Center for Atmospheric Research, Boulder, Colo

A supersonic magnus moment is shown to exist on a cruciform missile whose fins are deflected into an aileron setting The effect is unusual in that it does not depend on interference, but rather on the normal forces on the two panels that are instantaneously perpendicular to the plane of the angle of attack The moment is negative, large, and increases as the Mach number decreases toward 1 This agrees with scanty data obtained in 1955 in the aeroballistic range

Introduction

IN 1955 Nicolaides and MacAllister[1] presented what may well have been the earliest unclassified magnus data for a finned missile (Fig 23 of Ref 1) These data were obtained for a configuration known as "the basic finner," which is shown in Fig 1 The model was gun launched in the free flight ballistic range at the Ballistic Research Laboratory The fins were canted slightly into an aileron deflection in order to induce the spin that is necessary for the existence of magnus effects The data obtained are plotted in Fig 2; they consist of the magnus moment coefficient derivative

Received October 7, 1963

* Staff Scientist, Laboratory of Atmospheric Sciences Member AIAA

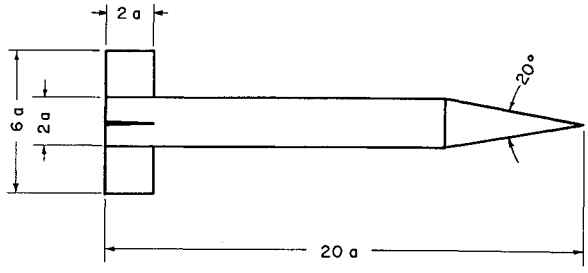

Fig 1 Basic finner configuration

$C_{M_{p\alpha}}$ as a function of Mach number M Interesting features of these data are the negative sign, the relatively large magnitude, and especially the large increase in $-C_{M_{p\alpha}}$ as the Mach number decreases toward 1 The author has not seen any explanation for these data The purpose of this note is to point out the existence of a simple, yet not well known, mechanism that gives rise to magnus moments of the indicated sign, magnitude, and general trend with Mach number

Known Causes for Magnus Effect

The classical magnus lift on a rotating cylinder and the magnus side force on a spinning missile of revolution at angle of attack both depend on boundary layer effects [2, 3] These effects are not expected to produce negative moments of the large magnitude observed in Fig 2 when the main flow becomes supersonic [4]

In Ref 5 the author has considered incompressible magnus effects on a missile with both wing and tail fins, showing that wing-tail vortex interference is a source of large, negative magnus forces and moments However, the basic finner discussed here does not have wing panels to shed vorticity ahead of the tail fins Moreover, even if the body shed sizable amounts of vorticity which could interact with the tail, there is no reason to expect the sensitive dependence on Mach number exhibited in Fig 2

Very recently Platou[6] has discussed supersonic magnus effects on a finned missile whose maximum fin span equals the maximum body diameter For such a configuration, wing-body interference is the primary source of magnus effects Yet wing-body interference on the basic finner should be fairly small because the body radius is only $\frac{1}{3}$ of the wing semispan [7, 8] Furthermore, during the tests which gave the data of Fig 2, the pitching and yawing motion was extremely small, and so the cross-flow velocities needed for wingbody interference must not have been large

Still another source of magnus effects on finned missiles is leading edge suction [9] For the rectangular panels of the

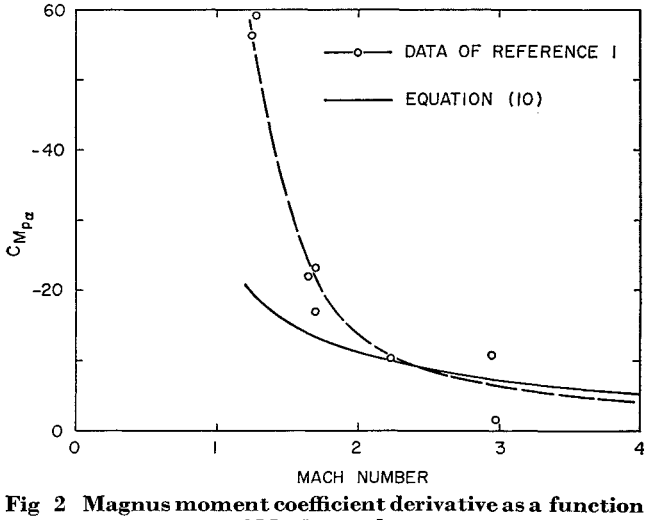

Fig 2 Magnus moment coefficient derivative as a function of Mach number